



## Measurement of Pulse Propagation Velocity, Distensibility and Strain in an Abdominal Aortic Aneurysm Mouse Model

Neekun Sharma<sup>\*,1,3</sup>, Zhe Sun<sup>\*,2,3</sup>, Michael A. Hill<sup>1,2,3</sup>, Chetan P. Hans<sup>1,2,3</sup>

<sup>1</sup>Division of Cardiovascular Medicine, University of Missouri

<sup>2</sup>Medical Pharmacology and Physiology, University of Missouri

<sup>3</sup>Dalton Cardiovascular Research Center, University of Missouri

### Abstract

An abdominal aortic aneurysm (AAA) is defined as a localized dilation of the abdominal aorta that exceeds the maximal intraluminal diameter (MILD) by 1.5 times of its original size. Clinical and experimental studies have shown that small aneurysms may rupture, while a subpopulation of large aneurysms may remain stable. Thus, in addition to the measurement of intraluminal diameter of the aorta, knowledge of structural traits of the vessel wall may provide important information to assess the stability of the AAA. Aortic stiffening has recently emerged as a reliable tool to determine early changes in the vascular wall. Pulse propagation velocity (PPV) along with the distensibility and radial strain are highly useful ultrasound-based methods relevant for assessing aortic stiffness. The primary purpose of this protocol is to provide a comprehensive technique for the use of ultrasound imaging system to acquire images and analyze the structural and functional properties of the aorta as determined by MILD, PPV, distensibility and radial strain.

### Keywords

Immunology and Infection; Issue 156; Abdominal aortic aneurysm; animal models of human disease; pulse propagation velocity; distensibility; strain; aortic stiffness; in vivo imaging

### Introduction

An abdominal aortic aneurysm (AAA) represents a significant cardiovascular disease characterized by a permanent localized dilation of the aorta exceeding the original vessel diameter by 1.5 times<sup>1</sup>. AAA ranks among the top 13 causes of mortality in the United States<sup>2</sup>. The progression of AAA is attributed to the degeneration of the aortic wall and elastin fragmentation, ultimately leading to aortic rupture. These changes in the aortic wall may occur without a significant increase in the maximal intraluminal diameter (MILD), thus

---

Correspondence to: Chetan P. Hans at HansCP@health.missouri.edu.

\*These authors contributed equally

Disclosures

The authors have nothing to disclose.

Video Link

The video component of this article can be found at <https://www.jove.com/video/60515/>

suggesting that MILD alone is not sufficient to predict the severity of the disease<sup>3</sup>. Therefore, additional factors need to be identified to detect initial changes in the aortic wall, which may guide early treatment options. The overall goal of this protocol is to provide a practical guide for assessing aortic functional properties using ultrasound imaging as characterized by measurements of pulse propagation velocity (PPV), distensibility and radial strain.

A well characterized experimental model to study AAA, first described by Daugherty and colleagues, involves subcutaneous infusion of angiotensin II (AngII) via osmotic pumps in *Apoe*<sup>-/-</sup> mice<sup>4</sup>. Precise measurement of MILD using ultrasound imaging has been instrumental in characterizing AAA in this mouse model<sup>5</sup>. Although histological changes during the development of AAA have been extensively studied, changes in the functional properties of the vessel wall such as aortic stiffness have not been well characterized. This protocol emphasizes the use of high-frequency ultrasound in combination with the sophisticated analyses as powerful tools for studying the temporal progression of AAA. Specifically, these approaches allow us to assess the functional properties of the vessel wall as measured by PPV, distensibility and radial strain.

Recent clinical studies in human subjects with AAA, as well as in the murine elastase-induced AAA model, suggest a positive correlation between aortic stiffness and aortic diameter<sup>6,7</sup>. PPV, an indicator of aortic stiffness, is accepted as an excellent measurement for quantifying changes in stiffness in vessel wall<sup>6,8</sup>. PPV is calculated by measuring the transit time of the pulse waveform at two sites along the vasculature, thus providing a regional assessment of aortic stiffness. We have recently demonstrated that increased aortic stiffness as measured by PPV, and at the cellular level as determined using atomic force microscopy, positively correlates with aneurysm development<sup>9</sup>. Further, the literature suggests that aortic stiffness may precede aneurysmal dilation and thus may provide useful information about regional intrinsic properties of the vessel wall during development of AAA<sup>10</sup>. Similarly, distensibility and strain measurements are the quantification tools to measure earlier changes of arterial fitness. Healthy arteries are flexible and elastic, whereas with increased stiffness and less elasticity, distensibility and strain is decreased. Here, we provide a practical guide and step by step protocol for the use of a high-frequency ultrasound system to measure MILD, PPV, distensibility and radial strain in mice. The protocol provides technical approaches that should be used in conjunction with the basic information provided by manuals for specific ultrasound imaging instruments and the accompanying video tutorial. Importantly, in our hands the described imaging protocol provides reproducible and accurate data that appear valuable in the study of the development and progression of experimental AAA.

To further demonstrate the utility of ultrasound imaging, we provide example images and measurements taken from our own studies aimed at using pharmacological approaches for preventing experimental AAA<sup>11</sup>. Specifically, notch signaling has been proposed to be involved in multiple aspects of vascular development and inflammation<sup>12</sup>. Using gene haploinsufficiency and pharmacologic approaches, we have previously demonstrated that Notch inhibition reduces the development of AAA in mice by preventing infiltration of macrophages at the site of vascular injury<sup>13,14,15</sup>. For the current article, using the

pharmacological approach for Notch inhibition we focus on the relationship between aortic stiffness and factors relating to AAA. These studies illustrate that Notch inhibition reduces aortic stiffness, which is a measure of AAA progression<sup>11</sup>.

## Protocol

The protocol for handling of mice and ultrasound imaging was approved by the University of Missouri Institutional Animal Care and Use Committee (animal protocol number 8799) and was conducted according to AAALAC International.

### 1. Equipment setup and preparation of mice

#### 1. Equipment setup

1. Turn on the ultrasound instrument, ultrasonic gel warmer and the heating pad.
2. Open the ultrasound program and enter the study name and descriptive information for each mouse.
3. Select the application as **General Imaging**.
4. Choose the appropriate transducer for abdominal imaging (Figure 1B,C). In this experiment, MS400 transducer is used.
5. Ensure anesthesia isoflurane and oxygen levels are adequate for each experimental session.
6. Clean the ultrasound animal imaging platform.

#### 2. Mouse preparation

1. Place the mouse cage on top of a heating pad (36.5 to 38.5 °C).
2. Gently hold the mouse by its tail base and place in the oxygen-filled isoflurane chamber.
3. Direct the isoflurane and oxygen flow to the induction chamber.
4. Turn on the isoflurane vaporizer and set the isoflurane level to 1–2% vol/vol. Turn on the oxygen tank pressure to 1–2 L/min.
5. After ~2 min, confirm the adequate depth of anesthesia by the absence of withdrawal reflexes upon pinching the foot pad of the mouse.
6. Next, turn off the induction chamber supply branch and turn on the branch directed to the anesthesia nose cone.
7. Transfer the mouse from the induction chamber to the ultrasound imaging stage and position the anesthesia cone over the nose of the animal.
8. Tilt the animal imaging platform around 10° to the lower right corner for optimal scanning (Figure 1B).

9. Put one drop of sterile ophthalmic solution in both eyes of mice to prevent drying under anesthesia.
10. Position the mouse in the supine position with its nose inserted into the anesthesia cone.
11. Apply the electrode gel to all four paws using a cotton swab and tape the paws to the copper leads on the animal imaging platform for electrocardiogram readings (Figure 1C).
12. Use clippers to shave hair at the imaging site and then apply depilatory cream to remove remaining fur. Leave for less than 1 min.
13. Gently wipe off the cream and hair with a damp paper towel.
14. Monitor the breathing and ensure that heart rate is maintained between 450–550 beats/min. If below this level, reduce the isoflurane flow and wait until the heart rate recovers.
15. Apply prewarmed ultrasonic gel (37 °C) to the prepared skin site and attach the transducer to its holder and lower down until it touches the gel (Figure 1C).

## 2. Ultrasound imaging of the abdominal aorta

1. Position the transducer horizontally (i.e., perpendicular to the midline of the mouse).
2. Smooth the ultrasonic gel and remove bubbles using the wood stick of a cotton swab.
3. Lower the transducer and place 0.5 – 1 cm below the diaphragm after touching the gel. Now start to observe the images.
4. Visualize the abdominal aorta in the short axis view (Figure 1C).

NOTE: B-mode is the default and most effective mode to anatomically locate the aorta and position the transducer. The abdominal aorta is identified by the presence of pulsatile flow using color Doppler and power Doppler modes in the short axis (i.e., the circumferential cross-section of the aorta). Adjust the micromanipulators on the animal stage and the transducer to bring the cross section of the aorta to the center of the image.

5. Gently rotate the transducer 90° clockwise, and slowly adjust the x-axis micromanipulator knob to visualize the aorta in long axis view (longitudinal section of the aorta).

NOTE: In many cases, gastro-intestinal gases may interfere with the image, or the aorta may not be at the optimal angle to allow a clear long axis view. Adjust the angle of the transducer slowly and horizontally until an acceptable long axis view is obtained. If problems persist, elevate the transducer, check for air bubbles under the transducer, slightly adjust the tilting angle of the animal stage, reapply gels, and repeat all the steps again.

6. Set the focus zone and depth at the region of the aorta using the **Focus Zone** and **Focus Depth** toggles, respectively. Adjust the **time gain compensation slider** manually to darken the lumen of the aorta to achieve an optimal contrast of the aorta wall.
7. Adjust the **y-axis manipulator** to visualize the branching points of the superior mesenteric and the right renal arteries. Use the right renal artery as a landmark to capture image of the suprarenal aorta (Figure 2A).
8. Record at least 100 frames of B-mode images on the suprarenal aorta.
9. Press cinestore to save the B-mode images.
10. Press **M-mode** button on the instrument keyboard to enable M-mode recording. Roll the cursor ball to bring the yellow indicator line to a normal aorta sections with clear vessel wall image, or to the sections where maximal diameter of aneurysm is observed.
11. Press the **SV/gate toggle** and adjust the cursor ball to ensure that vessel walls are included in the measurement bracket. Press **update** to record M-mode measurements and press **cinestore** to capture (Figure 2A,B).

NOTE: Maximal diameter of the aneurysm may not be in the same imaging plane as the optimal long axis view of the aorta. Adjust the x-axis manipulator knob slightly for each M-mode measurement to ensure that the MILD of each section is captured.

12. To obtain ECG-gated Kilohertz Visualization (EKV) images, press the **B-mode** button to go back to B-mode recording.

NOTE: If the images are not sharp, adjust the x-axis manipulator to achieve the sharpest image of upper wall of the lumen over a section length (i.e., > 6 mm).

13. Press **Physio Settings** button on the keyboard and select **Respiration Gating**. Adjust the gating **Delay** and **Window** manually to record the data only during the flatter parts of the respiration wave. The recording sections will be shown as colored blocks on the tracing of the respiration wave.

NOTE: Without the adjustment of the respiration gating, the EKV images will be blurred due to the normal movement of animal during breathing.

14. Press **EKV button** to enable the EKV mode. In the appropriate menu, select **Standard Resolution** and **frame rate 3000 or higher**. Select proceed to record **EKV images**. Press **cinestore** to save the images. Use EKV mode image to obtain measurements of pulse propagation velocity (PPV), distensibility and radial strain.

NOTE: EKV recording may fail if there are abnormal fluctuations in respiration, animal is respiring too rapidly, or frame rates settings are too high. In those case, set the frame rate lower and wait for the animal respiration to stabilize. Setting the frame rate at 3000 is usually appropriate for both mice and rats.

### 3. Post-imaging steps

1. Gently wipe the ultrasonic gel from the abdominal area of the mouse with a paper towel moistened with warm water.
2. Place the mouse back in its home cage on a heating pad.
3. Turn off the isoflurane machine, clean the animal imaging platform and transducer with damp wipes.
4. Transfer the image data collected during the ultrasound scan to the hard drive.
5. Turn off the ultrasound instrument.
6. After the mouse recovers from anesthesia and is alert, remove the heating pad and return the cage to the animal housing rack.

### 4. Analysis of abdominal aortic images

1. Analysis of M-mode images to measure MILD
  1. Open the ultrasound program and enter the study name and descriptive information for each mouse.
  2. Open the ultrasound data in the analysis software and open the M-mode image and pause the heartbeat.
  3. Click on **Measurements**.
  4. Select the **vascular package** from the drop-down options. Click on **Depth** and draw a line across the aortic lumen extending from inner wall to wall (Figure 2C,D).

NOTE: For consistency, the measurements should be taken at the systolic phase of the cardiac cycle when the aorta is maximally expanded. Draw three lines across three different heartbeats to obtain accurate and average measurements of MILD. In AAA, the measurements are taken at the maximal dilatation of the aorta. It is also advisable to fast the animals 4–6 h prior to collecting images to avoid interference from bowel motility and ensure image clarity.

2. Analysis for pulse propagation velocity (PPV)
  1. Open the EKV image and pause the heartbeat.
  2. Open a new window on the analysis software (e.g., Vevo Vac) by clicking on the name icon.
  3. Click on the **PPV option** (arrow in Figure 3D). A small window will further appear with the image of the aorta.
  4. Draw a rectangular box by clicking on the upper vessel wall and dragging the pointer for about 4 mm covering both the walls of the suprarenal aorta.

NOTE: Keep the length of the box consistent (~4 mm) for all the images. The user can adjust the rectangular box by rotating to align the

box and selecting the line then dragging to a new position on the vessel being analyzed to obtain the most appropriate and clear inflection of the pulse wave. The vertical lines of data from the rectangle will be displayed and identified as the Left (top image) and Right (bottom image) on the ROI. For a better visualization of the inflection of the pulse wave, it is sometimes useful to draw the box only on the upper wall as shown in Figure 3. The software will automatically calculate the PPV (m/s). However, it's always better to manually adjust the purple lines to set the exact inflection point on the pulse waves and PPV will change accordingly.

5. Finally, select the **Accept** command to save the PPV values. Export the figures and the data to the data storage drive.
3. Analysis for distensibility and radial strain
    1. Open the EKV image and pause the heartbeat.
    2. Click on the software icon. The software will open a new window.
    3. Click on the **trace new ROI** and draw a rectangular box on the both walls of the vessel. The software will automatically trace the upper and lower walls of the vessel. The user can adjust the trace to align on the wall by clicking on green points (Figure 4A,B).
    4. Now Accept the trace. The software will calculate the distensibility (1/Mpa) in the selected ROI.
    5. For the radial strain measurement, select the appropriate strain option from the menu bars on the top left. The images for radial strain and tangential strain will open.
    6. Obtain the value for radial strain (%) by moving the cursor on the peak of the curve. Export the data as images or in video format (Figure 4A,B).

### Representative Results

Representative M-mode images of the normal and aneurysmal abdominal aorta from mice are shown in Figure 2A and Figure 2B, respectively. The suprarenal abdominal aorta is identified by its location next to right renal artery and the superior mesenteric artery (Figure 2A). Representative images used for the calculation of MILD, at three different heartbeats of the systolic cardiac cycle, in normal and aneurysmal aorta are shown in Figure 2C,D respectively. In the situation where an aortic aneurysm has developed, the luminal diameter is determined by drawing a perpendicular yellow line between the two inner edges of the lumen at the area of maximal dilation (Figure 2B). Three independent measurements are typically averaged to determine an accurate intraluminal diameter.

Representative EKV images of the abdominal aorta used in analysis of PPV are shown in Figure 3. PPV is calculated by drawing a rectangular box on the luminal wall of suprarenal aorta (Figure 3E) and adjustment of the purple vertical lines of data obtained from the

rectangular box (Figure 3F). The purple lines should be adjusted to set the inflection point of the pulse waves. Representative EKV images of the abdominal aorta suitable for analysis of distensibility and radial strains are shown in Figure 4. Distensibility and radial strain are calculated by tracing the luminal walls of the suprarenal aorta as shown in Figure 4E. The value for distensibility (1/MPa) is obtained by choosing the distensibility/elasticity option from drop down menu of the box (red arrow, Figure 4F). The radial strain (%) is obtained by choosing the radial strain option (Figure 4G) and moving the cursor to the peak of the radial strain graph (Figure 4H).

We have validated the significance of PPV in the AngII-induced mouse model of AAA and further examined the therapeutic potential of a Notch inhibitor (N-[N-(3,5-difluorophenacetyl)-L-alanyl]- (S)-phenylglycine t-butyl ester; DAPT) on the progression and stability of pre-established AAA. Specifically, all these aneurysm studies were performed on 8–10 weeks old *Apoe*<sup>-/-</sup> male mice following infusion of AngII by published protocols<sup>4,13</sup>. At day 28 of AngII infusion, mice were randomly divided into two groups and were administered vehicle or DAPT (10 mg/kg) until sacrifice at day 56<sup>13</sup>. Transabdominal ultrasound imaging showed a progressive increase in the MILD, PPV, and a decrease in distensibility and radial strain in response to AngII at day 28 (Figure 5A–E). AngII infusion marginally increased MILD from day 28 to 56 and DAPT did not significantly change MILD compared to AngII alone (Figure 5A and Figure 5B). However, PPV increased progressively with AngII infusion at from day 28 to day 56 and DAPT significantly decreased further increases in PPV at day 56 (Figure 5C). Distensibility and radial strains, parameters to assess the elasticity of the vessel wall were decreased with AngII infusion while DAPT showed no significant effect (Figure 5D and 5E). It is important to appreciate that PWV correlated strongly with MILD at day 28 ( $R^2=0.51$ , Figure 5F), whereas at day 56, the correlation was relatively weak ( $R^2=0.22$ ) (Figure 5G). Aortic stiffness in AAA is primarily associated with changes in aortic wall architecture. Histologically, AngII infusion increased collagen degradation and proteolytic activity in the medial layer of the aorta (Figure 5H, **top row**). DAPT treatment minimized such changes in the ECM degradation (Figure 5H, **bottom row**).

## Discussion

Ultrasound imaging provides a powerful technique for determining functional properties of the aorta through measurements of PPV, distensibility and radial strain. These measurements are particularly instructive for studying mouse models of AAA and the *in vivo* approach allows for collection of longitudinal data that is potentially important to understanding temporal development of the aortic pathology. Specifically, measurements of *in vivo* aortic stiffness are determined locally in the abdominal aorta by PPV, distensibility and radial strain by analyzing EKV data and are considered as an independent risk factor for AAA instability<sup>16</sup>. The techniques described in these protocols are relatively straight forward and take only 8–10 min to obtain image sets from one mouse. All images should preferably be collected by a single operator using well-defined and consistent landmarks to generate reproducible and precise data.



There are potential factors that require technical expertise for the applications of these tools. For example, firstly, PPV may not solely reflect the degree of AAA development in the local arterial wall because it is an indirect measure of regional arterial stiffness. Secondly, it can be difficult to accurately measure PPV if the intimal wall is damaged. Third, it can be challenging to obtain sharp resolution images without expertise in operating the instrument. Some of these concerns have been addressed in recent versions of ultrasound imaging systems where speckle noise and artifacts are reduced, while preserving and enhancing data acquisition for small animal studies.

The focus of techniques used in the past (Doppler, microangiography, magnetic resonance imaging) to determine aortic stiffness were limited to two-dimensional images. PPV calculated from the ultrasound imaging has been emerging as a reliable and reproducible method to determine aortic stiffness and seems to be independent of arterial pressure<sup>9,17</sup>. It is important to note that the prevailing definition of AAA using maximal diameter as a standard index does not always reliably correlate with clinical observations. For instance, small aneurysms may rupture while some large aneurysms tend to remain stable<sup>18,19,20</sup>. Aortic stiffening is an early change generating aortic wall stress that triggers aneurysmal growth, and remodeling<sup>10</sup> and has been strongly correlated with Mmp2 and Mmp9 in mouse models of AAA<sup>10</sup>. Thus, in addition to the diameter of the aorta, functional analyses may provide important information to assess the progression and stability of AAA.

Using these protocols, we have examined the therapeutic potential of a potent pharmacological Notch inhibitor (2S-N-[(3,5-Difluorophenyl) acetyl]-L-alanyl-2-phenylglycine 1,1-dimethylethyl ester; DAPT) on the progression and stability of pre-established AAA using an AngII-induced mouse model of AAA<sup>11</sup>. Transabdominal ultrasound imaging showed a progressive increase in the MILD, PWV, and a decrease in distensibility and radial strain in the *ApoE*<sup>-/-</sup> mice in response to AngII than controls at day 28. No further increase in MILD was observed beyond day 28 till day 56 (Figure 5). However, PPV increased progressively and was significantly higher at day 56 compared to day 28. With the inhibition of Notch signaling by DAPT, MILD mice was not significantly different from AngII alone at day 56. Interestingly, DAPT prevented further increase in PPV such that it was significantly lower than AngII at day 56 (Figure 5C). DAPT treatment did not significantly affect distensibility or radial strain (Figure 5D,E). Interestingly, PPV correlated strongly with MILD at day 28 ( $R^2=0.51$ ), whereas at day 56, the correlation was relatively weak ( $R^2=0.22$ ; Figure 5F). These changes in the aortic stiffness were reflected in the increased collagen degradation and proteolytic activity with AngII and the attenuation by DAPT (Figure 5H). This example study highlights the potential value of ultrasound-based aortic stiffness measurements in understanding the time-course and predictability of both AAA progression and stability.

Further, the ultrasound based approach appears valuable in assessing the potential role for pharmacological interventions, particularly in stages that are likely to be independent of changes in intra-luminal diameter (i.e., beyond the expectation for actual regression). In summary, detailed understanding and usage of such technology will benefit in evaluating the prognosis of AAA at an early stage of the disease for effective therapeutic interventions.

## Acknowledgments

This work was supported by R01HL124155 (CPH) and funding from the Research Institute at the University of Missouri to CPH.

## References

1. Wanhainen A How to Define an Abdominal Aortic Aneurysm — Influence on Epidemiology and Clinical Practice. *Scandinavian Journal of Surgery*. 97, 105–109 (2008). [PubMed: 18575024]
2. Benjamin EJ et al. Heart Disease and Stroke Statistics—2018 Update: A Report From the American Heart Association. *Circulation*. 137, e67–e492 (2018). [PubMed: 29386200]
3. Xu J, Shi G-P. Vascular wall extracellular matrix proteins and vascular diseases. *Biochimica et biophysica acta*. 1842, 2106–2119 (2014). [PubMed: 25045854]
4. Daugherty A, Manning MW, Cassis LA Angiotensin II promotes atherosclerotic lesions and aneurysms in apolipoprotein E-deficient mice. *Journal of Clinical Investigation*. 105, 1605–12 (2000).
5. Au - Sawada H et al. Ultrasound Imaging of the Thoracic and Abdominal Aorta in Mice to Determine Aneurysm Dimensions. *Journal of Visualized Experiments*. e59013 (2019).
6. Raaz U et al. Segmental Aortic Stiffening Contributes to Experimental Abdominal Aortic Aneurysm Development. *Circulation*. 131, 1783–1795 (2015). [PubMed: 25904646]
7. van Disseldorp EMJ et al. Influence of limited field-of-view on wall stress analysis in abdominal aortic aneurysms. *Journal of Biomechanics*. 49, 2405–2412 (2016). [PubMed: 26924662]
8. Miyatani M et al. Pulse wave velocity for assessment of arterial stiffness among people with spinal cord injury: a pilot study. *Journal of Spinal Cord Medicine*. 32, 72–78 (2009).
9. Sharma N et al. Deficiency of IL12p40 (Interleukin 12 p40) Promotes Ang II (Angiotensin II)-Induced Abdominal Aortic Aneurysm. *Arteriosclerosis, Thrombosis, and Vascular Biology*. 39, 212–223 (2019).
10. Raaz U et al. Segmental Aortic Stiffening Contributes to Experimental Abdominal Aortic Aneurysm Development. *Circulation*. 131, 1783–1795 (2015). [PubMed: 25904646]
11. Sharma N et al. Pharmacological inhibition of Notch signaling regresses pre-established abdominal aortic aneurysm *Scientific Reports*. (2019).
12. Bray SJ Notch signalling: a simple pathway becomes complex. *Nature Reviews Molecular and Cell Biology*. 7, 678–89 (2006). [PubMed: 16921404]
13. Hans CP et al. Inhibition of Notch1 signaling reduces abdominal aortic aneurysm in mice by attenuating macrophage-mediated inflammation. *Arteriosclerosis, Thrombosis and Vascular Biology*. 32, 3012–23 (2012).
14. Cheng J, Koenig SN, Kuivaniemi HS, Garg V, Hans CP Pharmacological inhibitor of notch signaling stabilizes the progression of small abdominal aortic aneurysm in a mouse model. *Journal of American Heart Association*. 3, e001064 (2014).
15. Hans CP et al. Transcriptomics analysis reveals new insights into the roles of Notch1 signaling on macrophage polarization. *The Journal of Immunology*. 200, 164.13 (2018).
16. Paraskevas KI et al. Evaluation of aortic stiffness (aortic pulse-wave velocity) before and after elective abdominal aortic aneurysm repair procedures: a pilot study. *Open Cardiovascular Medicine Journal*. 3, 173–175 (2009).
17. Fortier C, Desjardins MP, Agharazii M Aortic-Brachial Pulse Wave Velocity Ratio: A Measure of Arterial Stiffness Gradient Not Affected by Mean Arterial Pressure. *Pulse*. 5, 117–124 (2017). [PubMed: 29761086]
18. Golledge J Abdominal aortic aneurysm: update on pathogenesis and medical treatments. *Nature Reviews Cardiology*. 16 (4), 225–242 (2019). [PubMed: 30443031]
19. Choksy SA, Wilmink AB, Quick CR Ruptured abdominal aortic aneurysm in the Huntingdon district: a 10-year experience. *Annals of the Royal College of Surgeons of England*. 81, 27–31 (1999). [PubMed: 10325681]

20. Luo F, Zhou X-L, Li J-J, Hui R-T. Inflammatory response is associated with aortic dissection. *Ageing Research Reviews*. 8, 31–35 (2009). [PubMed: 18789403]

Author Manuscript

Author Manuscript

Author Manuscript

Author Manuscript

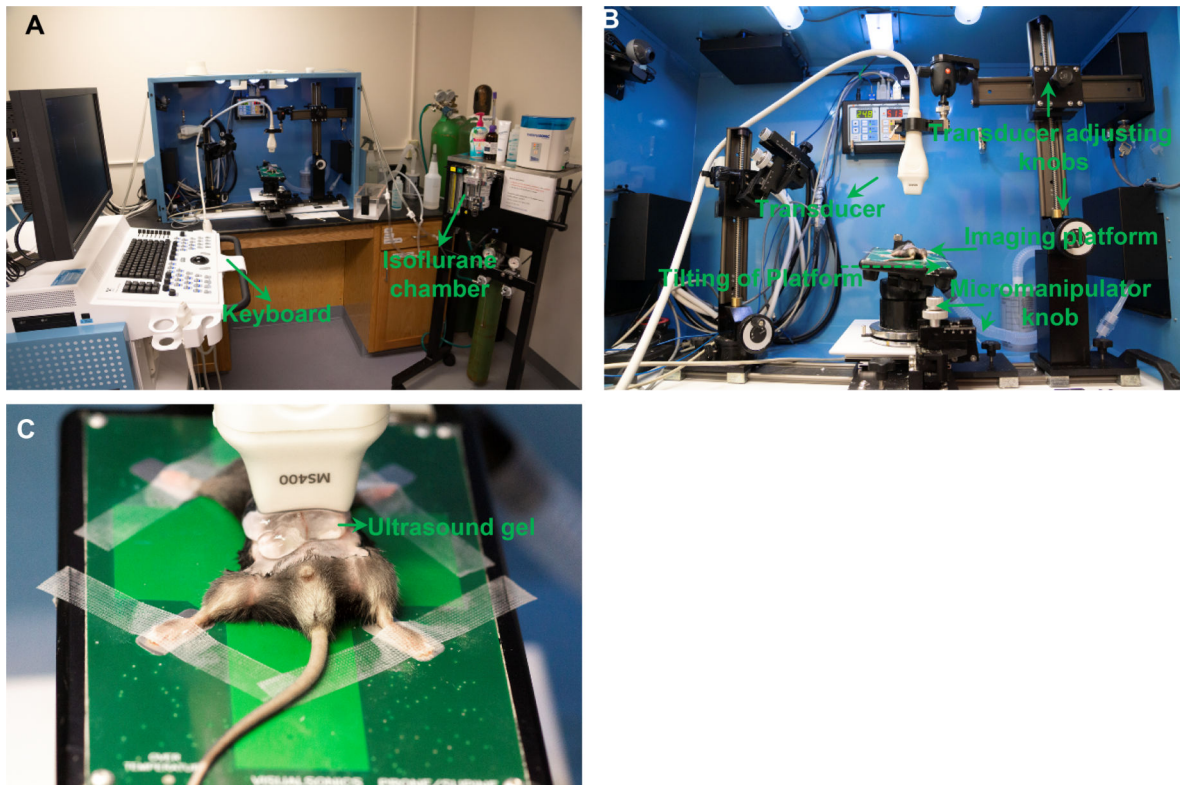


**Figure 1: Setup of the instrument.**

(A) Overall view of the ultrasound machine along with induction chamber for anesthesia and gel warmer. (B) Close up view of the imaging platform and the transducer system. (C) The view of the transducer placement while capturing short axis image of the abdominal aorta..

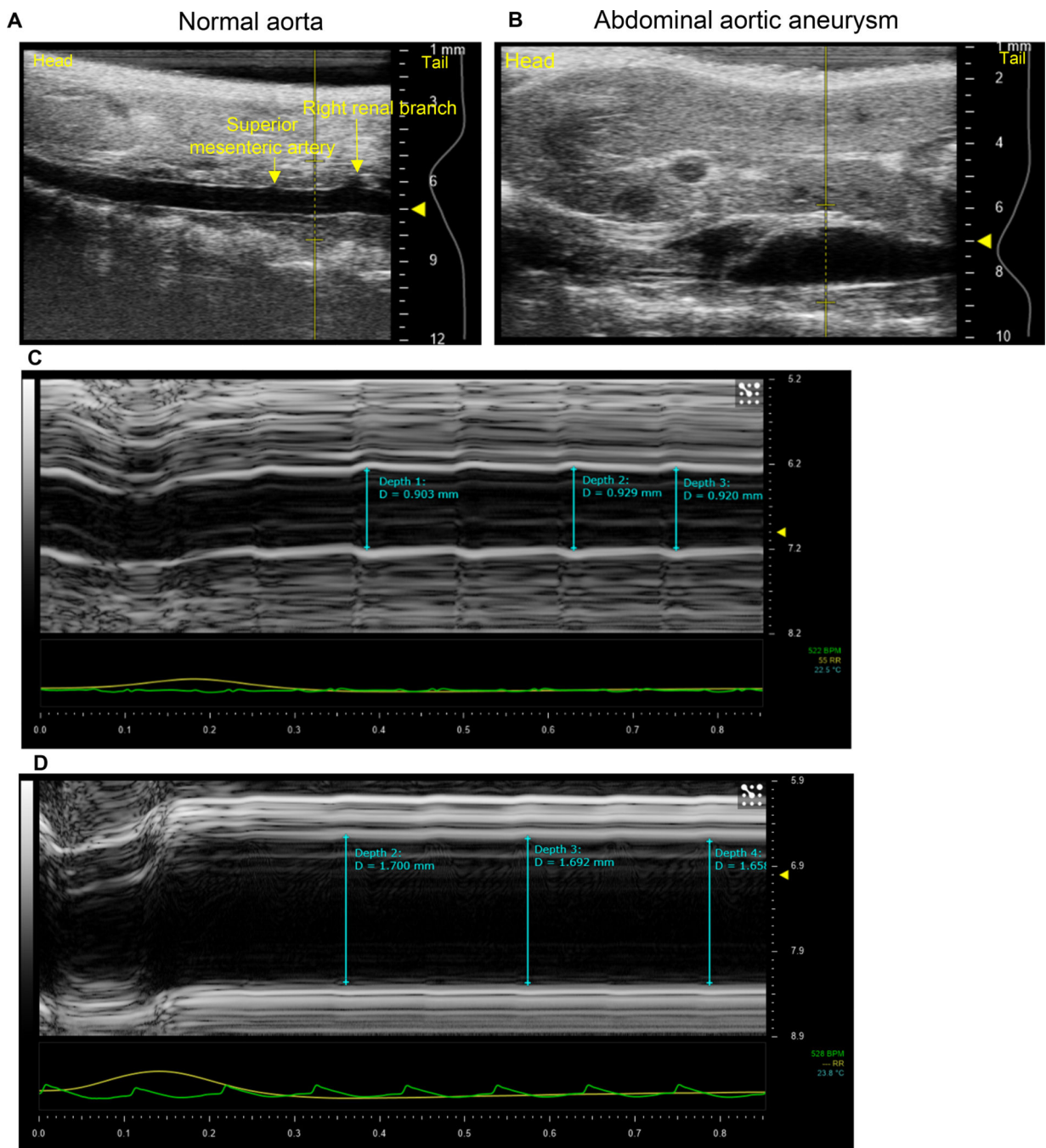


**Figure 2: Analysis of M-mode images for obtaining maximal intraluminal diameter (MILD).** The M-mode images of normal aorta (**A**) and aorta with abdominal aortic aneurysm (**B**) from mice are shown. (**C**) and (**D**), MILD drawn at systolic phase of the cardiac cycle in the suprarenal aorta of normal mice (**C**) and mice with AAA (**D**). Measurements at three different heartbeats are taken as shown and the average value is calculated..

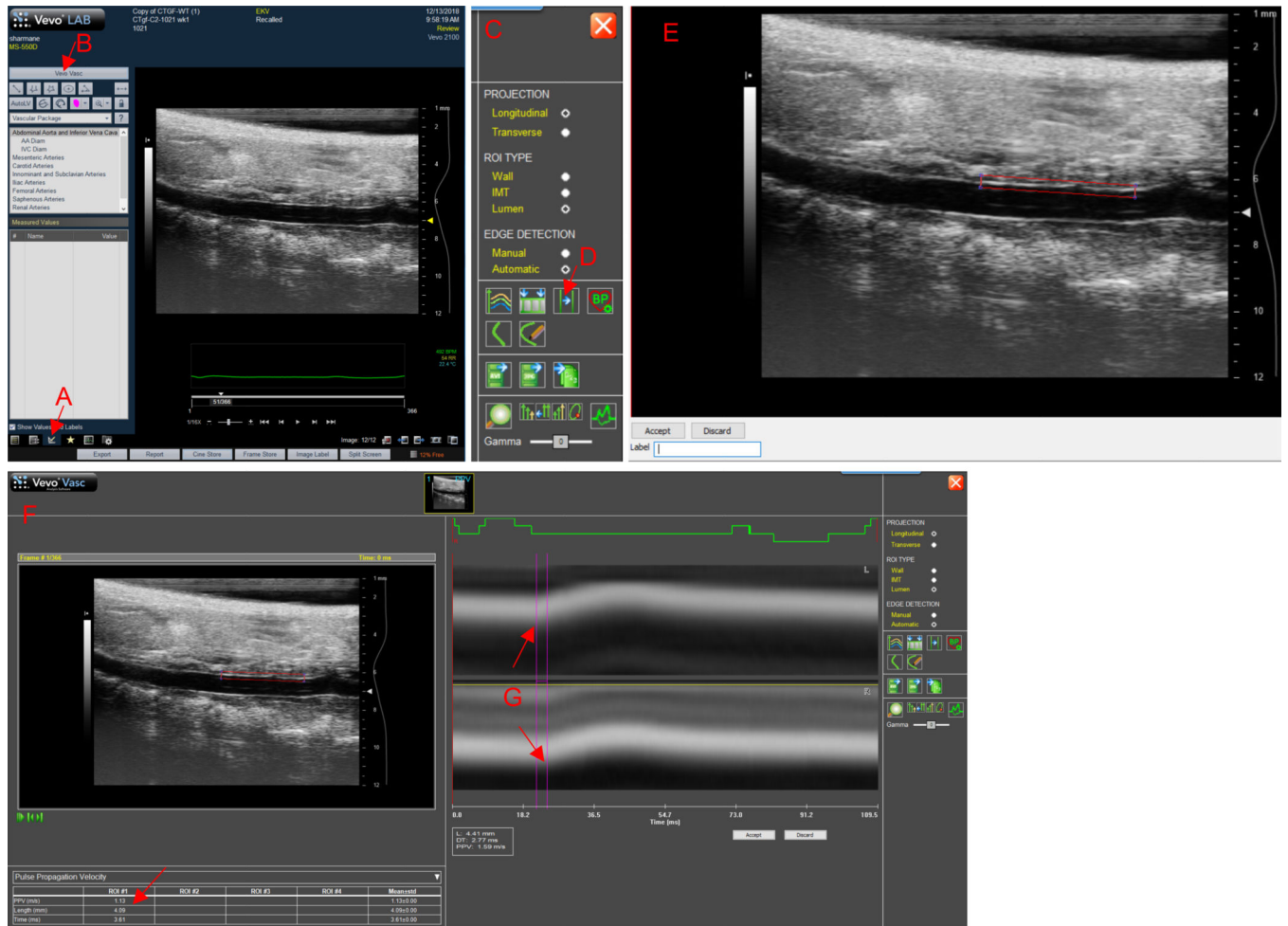


**Figure 3: Analysis of EKV images for obtaining pulse propagation velocity (PPV).** EKV images collected from normal mouse aorta. Analysis is done by clicking on measurements (A) and the software icon (B). A new window will appear with the icons on the right side, as shown in C. Now, click on PPV (D) and again, a small window will appear (E). Draw a rectangular box on the upper wall of the lumen as shown in E and click accept. The PPV value will be obtained as shown in F (arrow). The purple lines is adjusted to set the inflection point of the pulse waves (G).

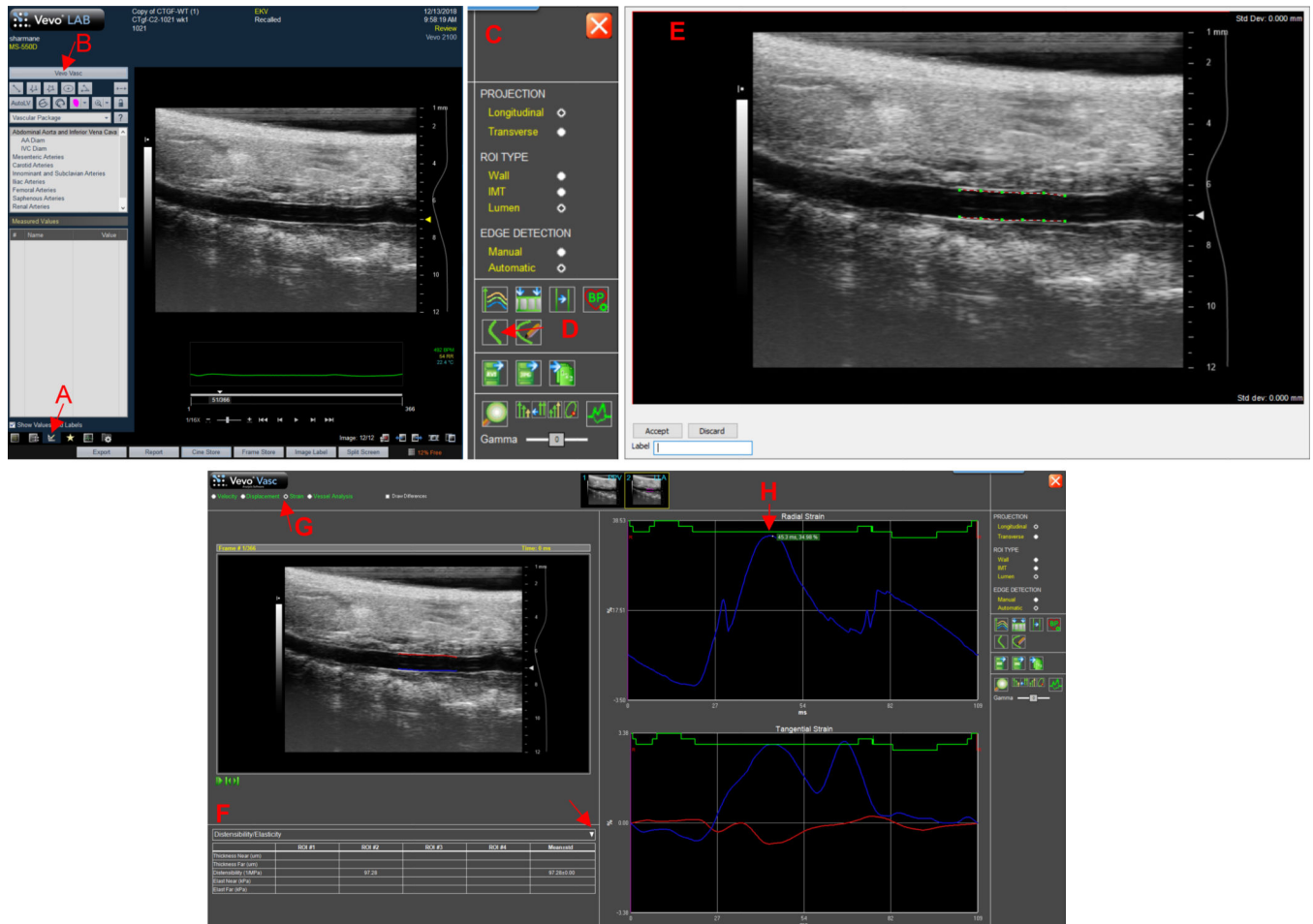


**Figure 4: Measurement of distensibility and radial strain.**

EKV images collected from normal mouse aorta. Analysis is done by clicking on measurements (A) and the software icon (B). A new window will appear with the icons on the right side, as shown in C. Now, click on trace new ROI (D), a new window will appear with traces on the upper and the lower wall of the lumen as shown in E and click accept. The value for distensibility will be obtained in table as show in the F. For strain, click on strain (G). The window will show the radial strain value (% , green highlighted box), as the cursor is placed on the peak of the radial strain graph (H).

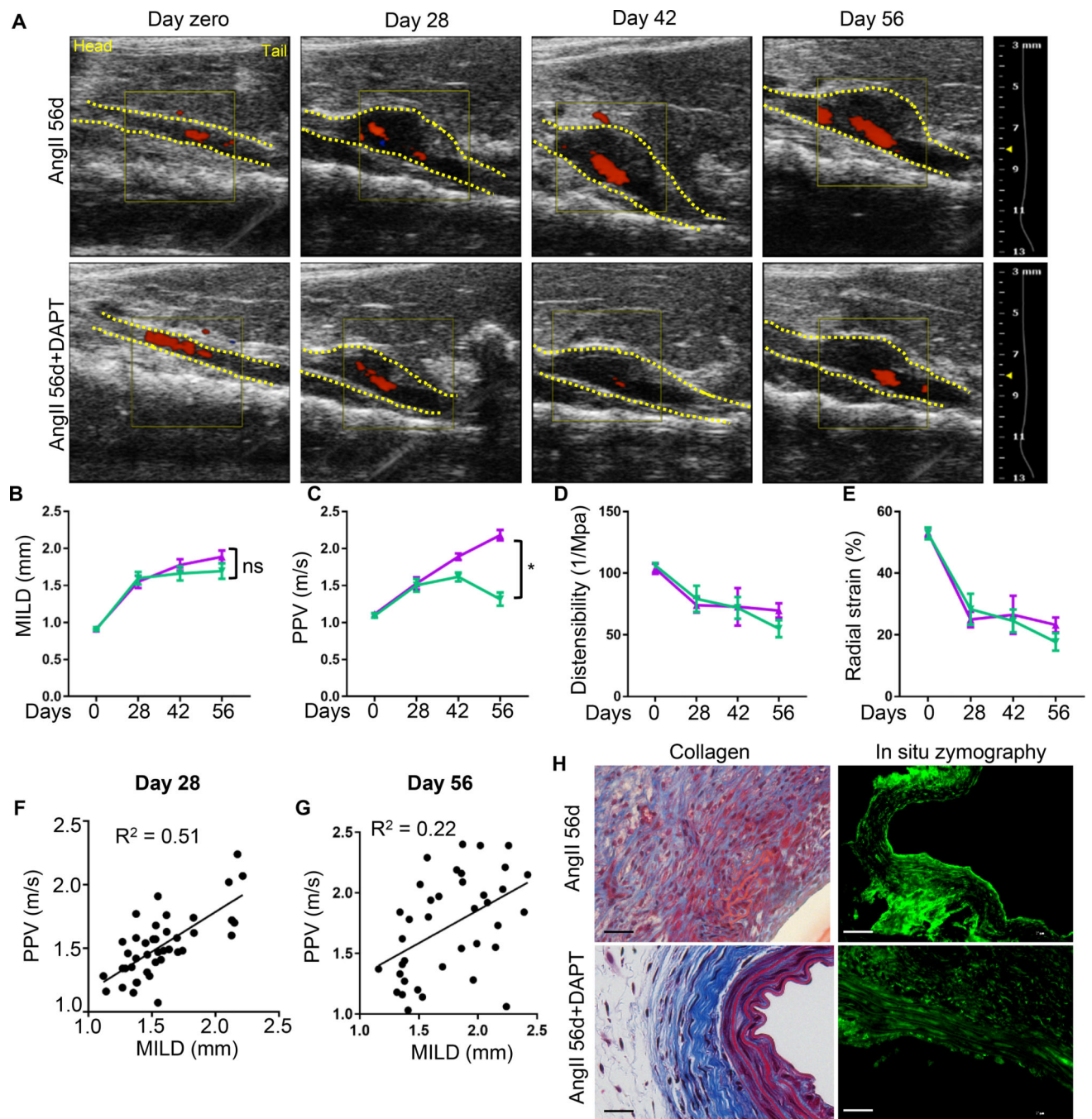


**Figure 5: PPV correlates with structural traits of aorta in the established AAA.**

(A) Representative transabdominal ultrasound images showing the MILD at day 0, 28, 42 and 56 of indicated experimental groups in *ApoE*<sup>-/-</sup> mice. DAPT was started at day 28. Dotted yellow lines outline the lumen. (B) Quantification of MILD in the indicated groups (purple and green color shows AngII + vehicle and AngII + DAPT treated mice respectively (n=16–18)). (C, D and E) PPV, distensibility and radial strain at various days of AngII and DAPT treatments (n=8). (F and G), Graphs showing Pearson's correlation between PPV and MILD at day 28 (F) and day 56 (G). (H) Representative histological images for collagen



staining (stained with trichrome and seen as blue staining) and proteolytic activity by in situ zymography with or without DAPT treatment at day 56. Tukey multiple comparisons test was used for data analysis. \* $P < 0.05$ ; ns = non-significant. Scale 50  $\mu\text{m}$  in H. This figure is adapted from Sharma et al. (2019), Scientific Reports (SREP-19-16491B)<sup>11</sup>.

Author Manuscript

Author Manuscript

Author Manuscript

Author Manuscript